Asian Research Journal of Mathematics

Volume 20, Issue 1, Page 1-15, 2024; Article no.ARJOM.111814
ISSN: 2456-477X

Modelling Mortality in Kenya

John K. Njenga [a*] and Isaac C. Kipchirchir [b]

[a] *University of Nairobi, P.O. Box 13187 - 00200, Nairobi, Kenya.*
[b] *Department of Mathematics, University of Nairobi, P.O. Box 30197 - 00100, Nairobi, Kenya.*

Authors' contributions

This work was carried out in collaboration between both authors. Both authors read and approved the final manuscript.

Article Information

DOI: 10.9734/ARJOM/2024/v20i1777

Open Peer Review History:
This journal follows the Advanced Open Peer Review policy. Identity of the Reviewers, Editor(s) and additional Reviewers, peer review comments, different versions of the manuscript, comments of the editors, etc are available here: https://www.sdiarticle5.com/review-history/111814

Original Research Article

Received: 16/11/2023
Accepted: 22/01/2024
Published: 23/01/2024

Abstract

This research work seeks to analysis the mortality trend experienced in Kenya over the sample period 1950 to 2021 using a multidimensional modeling framework. Life table functions, namely; life expectancy, survival function and age at death distribution are applied to depict mortality characteristics. Life expectancy and survival rate have significantly improved. There has been a shift in mortality status from a high mortality population, to an intermediate stage and mortality risk factors have increased across age. Mortality concentration curve and index within the Lorenz curve and Gini coefficient framework are used to analyze the lifespan inequality. Lifespan inequality is high with negligible improvements over time. Gompertz force of mortality is then estimated, which is statistically significant at 5% level. Deaths at exact age 25 is about 35 per ten thousand, with the rate death rate increasing by 6.09% per year starting from age 25. Under the assumptions of stable population, where the mortality and fertility functions are independent of time, Malthusian parameter is estimated which is less than zero for selected years. Kenya is a shrinking population and death rate decrease with increase in Malthusian parameter. Finally, to model long-term mortality rate forecast, Lee-Carter model is estimated. The model is statistically significant at 5% level explaining 78.4% of the variations. Expected life expectancy at a given age is projected to increase, with life expectancy at birth in 2030 and 2071 being 65.6 and 70.5 years respectively.

**Corresponding author: E-mail: jnonjenga@gmail.com;*

Keywords: Life expectancy; mortality rate; life table; age specific mortality rate.

1 Introduction

Globally in the last century, the has been a reduction in mortality and increase in life expectancy. These improvement have been attributed to awareness of health behavior and modernization of health infrastructure (Roser et al. [1]). Global life expectancy at birth in 2021 is 71 years with the least developed countries lagging behind by 7 years (UN WPP 2022). Covid-19 pandemic period between late 2020 and 2021 resulted to slowed life expectancy improvement in the world. Life expectancy at birth in the sub-Saharan Africa is 59.7 for both sexes. Female lead with 61.6 years as compared to males at 57.8 years. Models for analyzing mortality rates are categorized into three groups, namely; expectation models, explanatory models and extrapolative models. Expectation models are based on the a demographer opinion while explanatory models are based structural analysis of cause of death. Extrapolative models are based on the past mortality trend. The latter models have an have an advantage in modeling long-term forecast as compared to former models.

Age specific period life table function are tools used to analyze mortality. The shape of age-at-distribution derived from the life table death density function, is used to describe variability of age at death, shift in modal age at death and any shift in mortality. The age-at death distribution is well summarized by the mean and variability. Mean is equivalent to life expectancy at birth while variability measures the dispersion around the mean. Modal age death corresponding to the maximum value of the density has become a better longevity indicator in low mortality population. (Canudas-Romo 2008 [2] ,Canudas-Romo 2010 [3], Ouellette and Bourbeauet [4],Horiuchi et al. 2013 [5] , Basellini and Camarda [6], Shang and Haberman [7] , Bergeron-Boucher et al. [8]). Survival curves dimensions are used in mortality analysis to determine highest normal life duration that exceeds modal age, death around the modal age and the proportion of survivors in population (Cheung et al. [9], Ebeling et al. [10]). Gini coefficient and Lorenz curve are are mortality concentration index and curve for inequality measure. Lorenz curve shows the spread of the disparity from the equality line while Gini coefficient quantify the area between line of equality and Lorenz curve. Shkolnikov [11] (2003) developed a framework of applying the two measure to evaluate life inequality. This techniques was been applied by Vaupel et al. [12] (2011) ,Giorgi et al. [13] 2017 and Zafeiris [14] 2023 in their disparity analysis. In mortality modeling and forecasting, the model developed by Lee and Carter [15] has been widely used. The model is time series based model for forecasting long-run age specific mortality. Age specific mortality is expressed as a function of unobserved time specific intensity index and an additional parameter dependent on age. The model has been applied in analyzing mortality rates in different countries such as; Chile (Lee and Rofman [16]), G7 countries (Tuljapurkar et al. [17]), Australia (Booth et al. [18], Carter and Prskawetz [19], and Booth and Tickle [20]), Sweden (Lundström and Qvist [21]), Spain (Debón et al. [22]), India (Chavhan and Shinde [23]), Malaysia (Ibrahim et al. [24]), China & Pakistan (Mubarik et al. [25]), Italy (Carfora and Orlando [26]) and Bangladesh (Fazle and Khan [27]).

The aim of this paper is to analysis the trend and model mortality in Kenya using multidimensional approach. This is achieved by analyzing the life table functions, determining lifespan inequality using mortality concentration curve and index, determining the force of mortality under Gompertz law, estimating the Malthusian parameter under the assumptions of stable population and estimating Lee-Carter mortality model to forecast life expectancy.

2 Methodology

2.1 Data

The source of data employed in this study is the UN (United Nation) WPP22 (world population prospect year 2022) [28]. The dataset consist of single year population and deaths for both male and female from 1950 to 2021. According to Keilman [29] research o the accuracy of UN world population projection using 12 set of population projection between 1950 and 1980, he observed a clear tendency over time towards accuracy improvements.

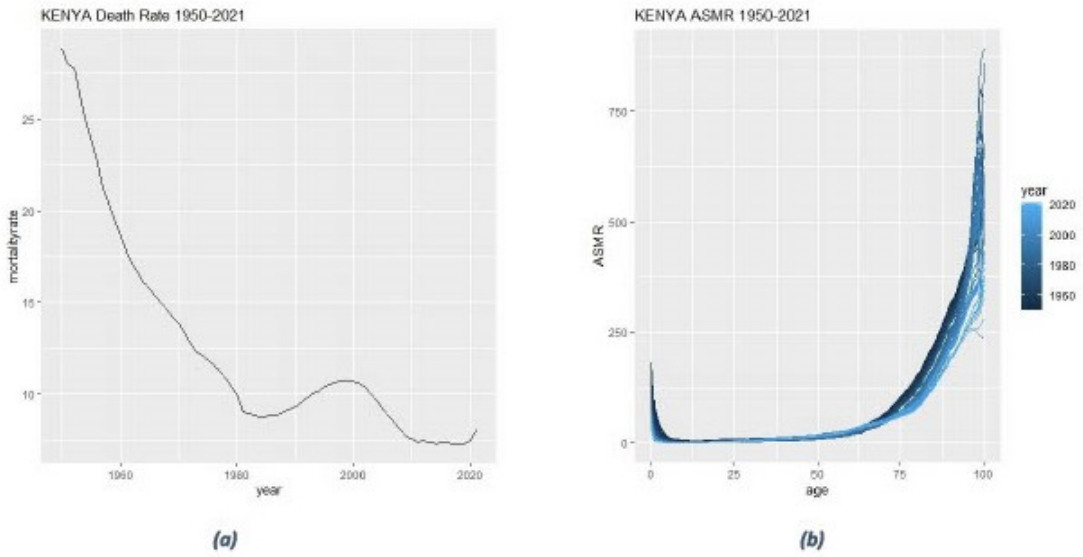

Fig. 1. Crude mortality rate plot

Crude mortality rate trend in Kenya is shown Fig. 1(a). Its evident that mortality rate has reduced over time. There was however a break in the decrease trend in the 1990s. Age specific mortality (ASMR) are analyzed to show clear variation in mortality across age and year as shown in Fig. 1(b). Infant mortality has sharply declined over time. From 6 years to 63 year, there has been less variability in ASMR over time. After 63 years, ASMR tends to increase though there has been a decrease in value over time. In the neighborhood of 100 years there is a lot of volatility over time.

2.2 Model

2.2.1 Life table function

A current life-table gives a cross section view of the survival and mortality experiences in a population by all ages. Life table functions are;

$$p_x = \frac{l_{x+1}}{l_x} \tag{2.1}$$

$$q_x = \frac{d_x}{l_x} \tag{2.2}$$

$$d_x = l_x - L_{x+1} \tag{2.3}$$

$$L_x = \int_x^{x+1} l_y dy \tag{2.4}$$

$$T_x = \int_0^{\omega - x} L_{x+t} dt \tag{2.5}$$

$$e_x = \frac{T_x}{l_x} \tag{2.6}$$

Where l_x is the number alive at exact age x, p_x is the probability of surviving from exact age x and $x+1$, q_x is the probability of dying between exact age x and $x+1$, d_x is the number of deaths between exact age x and $x+1$, L_x is number of person-years lived between exact age x and $x+1$, T_x is total number of person-years lived from exact age x, ω is the maximum attainable age and e_x is the life expectancy at exact age x.

Age survival curve is the plot of the share of individual expected to survive upto a certain age, which is obtained from survival function. Age at death distribution is a plot of the death function. The plot of the life expectancy, survival function and the death function are as shown in Fig. 2.

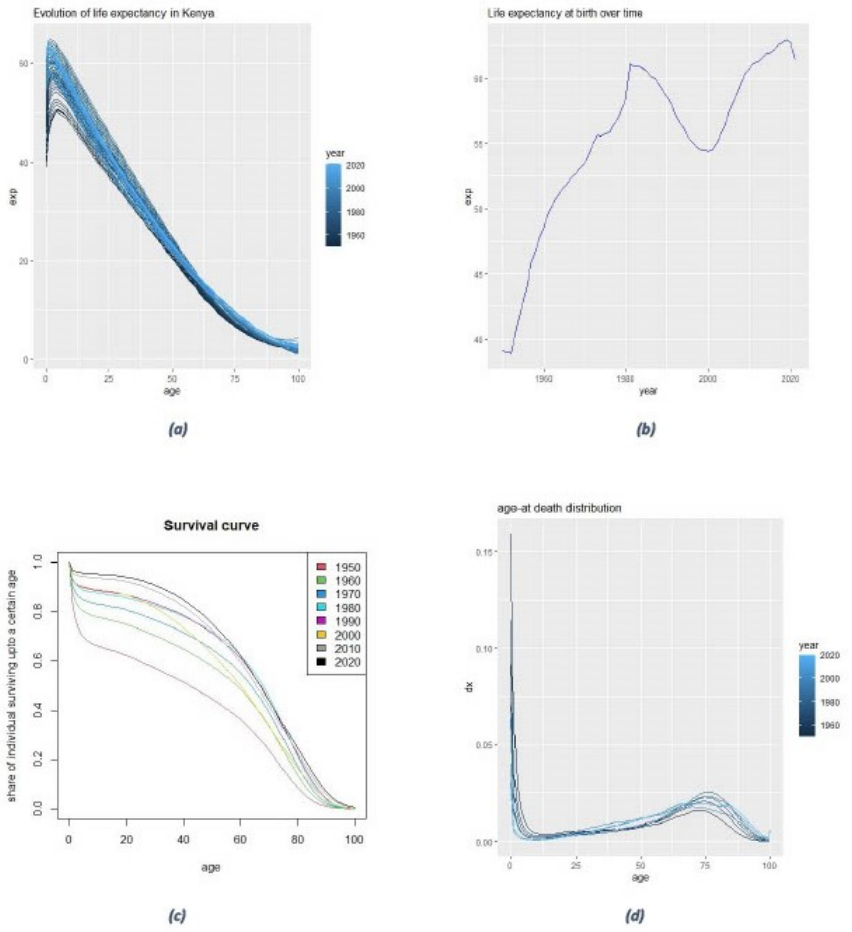

Fig. 2. Life table function plot

Fig. 2(a) show the evolution of life expectancy over time in Kenya. Life expectancy at birth has increased in the recent years to more than 62 years as compared to 1950s to 1970s that was within the range of 40 to 55 years. Life expectancy from age 1 to 62 has declined in the recent years as compared to early 1980s and has improved as compared to 1950 to 1960. From the age of 63 , life expectancy has increased over time. Fig. 2(b) show the trend in life expectancy at birth of the years. There is a continuous increase in life expectancy at birth with breaks in the trend as from 1990 to 2000 and around the Covid-19 pandemic period. Less than half of the

population in mid-20th century made past 50 years as shown in Fig. 2(c). In contrast, more than 80% of the population in 2020 were expected to live longer than 50 years.

The distribution of age at death is characterized by two mode; younger mode for infant and older age mode for adult. In the early years, Kenya was higher mortality population with younger mode being greater than older age mode, as shown in Fig. 2(d). This was characterized by infant mortality of 150 death per 1000 in 1950. However the trend has improved with the recent years having low younger age mode and low infant mortality of approximately 26 death per 1000 in the year 2020. The older age mode has slightly shifted over years. The gap between the younger mode and older age mode has also reduced over time, for example year 2020 younger age mode being 0.026 which is equivalent to older age mode of 0.024. This indicates a progress shift in mortality from high mortality population to intermediate status. The dispersion of the age at death distribution has also reduced with time. There exist a heavy tail on both side of the distribution in the recent year as compared to 1950s and 1960s. The mortality risk factors tends to be wide spread across age recently as compared to early years The modal age at death corresponding to the peak of the distribution has slightly varied over time ranging from 73 to 76 years in 2020 and 1980 respectively.

2.2.2 Mortality concentration curve and index

Mortality concentration curve is the best technique of analyzing lifespan inequality. Concentration curve is associated with Lorenz curve and while the concentration index is associated with the Gini index. Lorenz curve when applied to demography shows person's year lived distribution that's the cumulative person years lived share as a function of the cumulative death number share. Lorenz curve, $y = L(p)$, has the following equations (Hanada [30]);

$$L(p) = \frac{1}{\mu}\int_0^p xf(x)dx \tag{2.7}$$

$$p = \int_0^x f(x)dx \tag{2.8}$$

Where $f(x)$ is a density function shown in equation (2.9) and μ is the expectation.

$$f(x) = \frac{d_x}{l_0} \tag{2.9}$$

From the density function, the cumulative death density function of person year lived x ($F(x)$) and the cumulative share of deaths with person lived less or equal to x ($\Phi(x)$) are expressed as shown in equation (2.10) and equation (2.11) respectively.

$$F(x) = 1 - \frac{l_x}{L_0} \tag{2.10}$$

$$\Phi(x) = \frac{T_0 - (T_x + xl_x)}{T_0} \tag{2.11}$$

The divergence between the diagonal and Lorenz curve indicates the variability in person year's lived. Perfect equality happens at only two end points

- $F(x) = 1, \Phi(x) = 1$ for $x = e_0$
- $F(x) = 0, \Phi(x) = 0$ for $\forall x, x \neq e_0$

Gini index is a measure of absolute value mean of the inter-individual difference in age at death, divide by life expectancy (Shkolnikov et al. [11]). It normally ranges from 0 to 1. For values close to 1 indicates greater

inequality. Gini index expresses the amount of space between perfect line of equality and the lorenz curve doubled. It's the area enclosed by $y = L(\,\mathrm{p}\,)$ and $y = x$ to the area of triangle $y = 0, y = x$ and $x = 1$

$$G = 2\int_0^1 (x - L(x))dx \tag{2.12}$$

Substituting x and $\mathrm{L}(\,x\,)$ in equation (2.12), and using the partial integration identity,

$$\frac{d(1 - F(t))}{dt} = -f(t) \tag{2.13}$$

, then Gini index is expressed as

$$G = 1 - \frac{1}{\mu}\int_0^\infty (1 - F(x))^2 dx \tag{2.14}$$

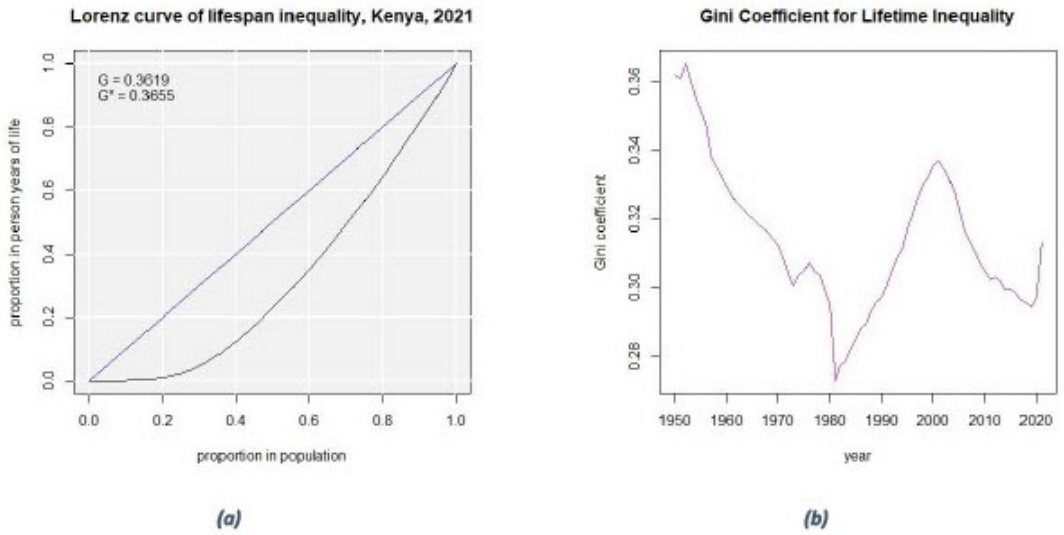

Fig. 3. Concentration curve plot

Considering year 2021 life table the Lorenz curve and Gini index are shown in figure 3(a). For those longest-lived 20% person claimed 32% of the total number of life years indicated by upper part of the curve. Short-lived 40% of persons claimed around 18% of all years of life shown at bottom of the curve. Gini index based on age specific mortality in 2021 is estimated to be 0.3619, indicating that person year lived from birth to death are less equally distributed. The Gini coefficient for the other years were calculated and plotted as shown in Fig. 3(b). There has been a slight improvement in lifespan disparity over time. The maximum Gini value is 36 in 1950 and the minimum value being 28 in the year 1980 when expressed as a percentage. Kenya is characterized as a population with high lifespan inequality that has not improved over time, commonly experienced in developing countries (Peltzman [31]).

2.2.3 Force of mortality

Force of mortality denoted as μ_x is the instantaneous death rate at exact age x. Its the ratio of rate of change in the number of survivors (l_x) at exact age x to the number of survivors (l_x), that is

$$\mu_x = \lim_{\delta x \to 0} \frac{l_x - l_{x+\delta x}}{l_x.\delta x} \tag{2.15}$$

which reduces to equation (2.16)

$$\mu_x = \frac{-1}{l_x} \lim_{\delta x \to 0} \frac{l_{x+\delta x - l_x}}{\delta x} \tag{2.16}$$

where μ_x ia also used for $\mu(x)$. Solving the limit, force of mortality is given as;

$$\mu_x = \frac{-1}{l_x} \frac{dl_x}{dx} \tag{2.17}$$

Gompertz [32] attributed death to either deterioration of the power to understanding destruction or chance. He stipulated that, the power of man to resist death (R_x) decreases at a rate proportional to the power itself, that is

$$\frac{dR_x}{dx} = -hR_x \tag{2.18}$$

where h is a positive constant. Integrating equation (2.18)

$$\int \frac{dR_x}{R_x} = -h \int dx \tag{2.19}$$

$$lnR_x = -hx + k \tag{2.20}$$

$$R_x = e^{-hx+k} \tag{2.21}$$

$$R_x = e^k . e^{-hx} \tag{2.22}$$

Since force of mortality is man's measure of susceptibility to death, Gompertz [32] also stipulated that

$$R_x = \frac{1}{\mu_x} \tag{2.23}$$

Thus equation (2.22) reduces to

$$\mu_x = e^{-k} e^{hx} \tag{2.24}$$

Both e^{-k} and e^h reduces to constants B and C respectively, thus equation (2.24) becomes;

$$\mu_x = BC^x \tag{2.25}$$

Constants B and C are estimated by expressing force of mortality (μ_x) in term of $l_x mh$. Applying chain rule for natural logarithm to equation (2.17)

$$\mu_x = \frac{-d}{dx} lnl_x \tag{2.26}$$

integrating both side of equation (2.26)

$$\int_0^y dlnx = \int_0^y -\mu_x dx \tag{2.27}$$

Solving the integral on the left hand side of equation (2.27), one obtains

$$ln(\frac{l_y}{l_0}) = -\int_0^y -\mu_x dx \tag{2.28}$$

Therefore

$$l_x = l_0 e^{-\int_0^x \mu_t dt} \tag{2.29}$$

From equation (2.25), then equation (2.29) reduces to

$$l_x = l_0 e^{-B\int_0^x -\mu_t dt} \tag{2.30}$$

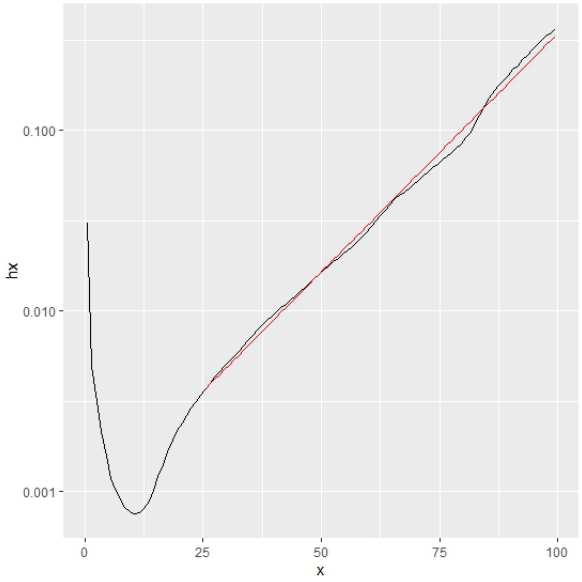

Fig. 4. Force of Mortality

Table 1. Gompertz force of mortality results

	a	Estimation	
	Estimate	Std. Error	P-value
(Intercept)	-5.6286523	0.0190883	2×10^{-16}
slope	0.0608969	0.0004408	2×10^{-16}
	R-Squared: 0.9962 F statistics: 1.908×10^4 on (1,73) DF p-value < 0.0001		

Solving the integral by substitution method where $z = c^t$,

$$l_x = l_0 e^{-\frac{B}{lnC}(C^x - 1)} \tag{2.31}$$

The age from 25 years is selected to model the force of mortality as it seems to be linear as shown in Fig. 4. The estimated parameter of the Gompertz model are shown in Table 1. The estimated Gompertz model is statistically significant at 5% level. From the model the values of constant B and C are 0.0609 and 0.0035 respectively. The constant C states that the deaths at exact age 25 is just about 35 per ten thousand, and the slope equivalent to B indicates the death rate increases by 6.09% per year starting at age 25.

2.2.4 Malthusian parameter

Malthusian parameter also known as the intrinsic rate of natural increase, denoted as r. Its defined as the rate of population increase that reproduce within discrete intervals of time and has generations that are not overlapping (Malthus [33]). It's based on stable population assumptions which state that; death rate,rate of increase, age distribution and birth rate are independent of time. Thus the respective mortality and fertility functions reduces as follow

$$c(a,t) = c(a) \tag{2.32}$$

$$\mu(a,t) = \mu(a) \tag{2.33}$$

$$d(t) = d = \int_0^{\omega} c(a)\mu(a)da \tag{2.34}$$

$$b(t) = b = \int_0^{\beta} c(a)m(a)da \tag{2.35}$$

where a is age, $c(a)$ is age distribution, $\mu(a)$ is force of mortality, $m(a)$ is the age-specific fertility rate for female births and $p(a)$ is the probability of surviving from birth to age a. The notation ma for $m(a)$ is also used. Consider stable population characteristic equation given as

$$\int_{\alpha}^{\beta} e^{-ra}p(a)m(a)da \ = 1 \tag{2.36}$$

where α and β are the mimimum and maximum ages of child bearing respectively.

Multiplying both side by the reciprocal of R_0 and solving using numerical method, equation (2.36) reduces as shown below

$$\frac{1}{R_0}\int_{\alpha}^{\beta} e^{-ra}p(a)m(a)da \ = \frac{1}{R_0} \tag{2.37}$$

$$r = \frac{lnR_0}{E(A)} \tag{2.38}$$

where

$$R_0 = \int p(a)m(a)da = \frac{1}{l_0}\int l_a m(a)da \tag{2.39}$$

is the net reproductive rate,

$$E(A) = \frac{1}{R_0}\int_a p(a)m(a)da \tag{2.40}$$

is the mean age of child bearing. , l_x is the number of survivors at age x and m_x is the is the female offsprings per female at an exact age x (age specific fecundity). If

- $r = 0$, a stationary population
- $r < 0$, a shrinking population
- $r > 0$, an expanding population

The effect of intrinsic rate on death rate is obtained by solving equation (2.34)as follows

$$lnd = ln\int_0^{\omega} c(a)\mu(a)da \tag{2.41}$$

$$\frac{dlnd}{dr} = \frac{dln}{dr}ln\int_0^{\omega} c(a)\mu(a)da \tag{2.42}$$

$$\frac{1}{d}\frac{d}{dr} = \frac{\int_0^{\omega}(\frac{d}{dr}c(a))\mu(a)da}{\int_0^{\omega} c(a)\mu(a)da} \tag{2.43}$$

Equation (2.43) finally reduces to

$$\frac{1}{d}\frac{d}{dr} = E(A) - E(A)_{death} \tag{2.44}$$

Where $E(A)_{death}$ is the mean age at death. Therefore,

$$\frac{d}{dr} = (E(A) - E(A)_{death})d \tag{2.45}$$

For

- E(A) $> E(A)_{death}$, d increase with r
- E(A) $< E(A)_{death}$, d decrease with r
- E(A) $= E(A)_{death}$, d does not change for a change in r

Table 2. Intrinsic rate of increase and related function results

	value(2021)	value(2000)	value(1980)
R_0	0.7261	0.5312	0.4120
$E(A)$	3128.705	2786.959	2719.373
r	-0.0001	-0.0002	-0.0003

Table 2. shows intrinsic natural rate of increase for three selected years, with all the three years having r less than zero. This implies that Kenya is a shrinking population. Intrinsic rate of natural increase has increased from 1980, though by a small margin. Since the age of child bearing is 15 to 49 years, then mean age of child bearing is less than the mean age at death which was shown under age-at death distribution section, to range between 72 to 75 years. This implies that death rate (d) decrease with increase in r. Kenya death rate has been reducing under stable population conditions as the intrinsic rate of natural increase improves.

2.2.5 Lee - Carter model estimation

Lee and Carter [15] developed a model that expresses natural logarithm of age-specific death rate as a linear function of unobserved specific period index with its parameters being dependent on age.

$$ln(m_{x,t}) = \alpha_x + \beta_x \kappa_t + \epsilon_{x,t} \tag{2.46}$$

where α_x and β_x are age dependent parameters, κ_t is a stochastic process dependent only on year of observation and $\epsilon_{x,t}$ is the error term.

The exponential of α_x is the general shape by age while β_x describe the rate of decline in response to change in κ ie

$$\frac{dln(m_{x,t})}{dt} = \beta_x \frac{d\kappa}{dt} \tag{2.47}$$

Where

- κ is linear in time: - implies each age specific mortality changes at its own constant exponential rate
- κ approaches $-\infty$: - implies each age specific mortality rates approaches zero. There is no negative death rates.

OLS method is used to estimate the parameter α_x, β_x and κ_t for $x = 1, 2, 3, \ldots, N$ and $t = 1, 2, 3, \ldots, T$, subject to boundary conditions

$$\sum_{x=1}^{N} \beta_x = 1 \quad and \quad \sum_{t=1}^{T} \kappa_t = 0 \tag{2.48}$$

The estimator of α_x is given as

$$\hat{\alpha_x} = \frac{1}{T}\sum_{t=1}^{T} ln(m_{x,t}) \tag{2.49}$$

The other parameter estimators are then obtained by singular value decomposition (SVD) of $N \times T$ matrix M, for

$$M_{x,t} = ln(m_{x,t}) - \hat{\alpha_x} \tag{2.50}$$

Under SVD, the solution is

$$M = UDV^T \tag{2.51}$$

Then, the estimator for parameter $beta_x$ and κ_t are given as:

$$\hat{\beta_x} = \frac{1}{c}U_{x,1} \quad and \quad \hat{\kappa_t} = c.D_{1,1}.V_{1,t} \tag{2.52}$$

where
$D_{1,1}$ is the largest singular value of M
$U_{x,1}$ is the entry value at (x,1) of U
$V_{1,t}$ is the entry value at (x,t) of V and
$c = \sum_{x=1}^{N} U_{x,1}$ satisfying the boundary conditions

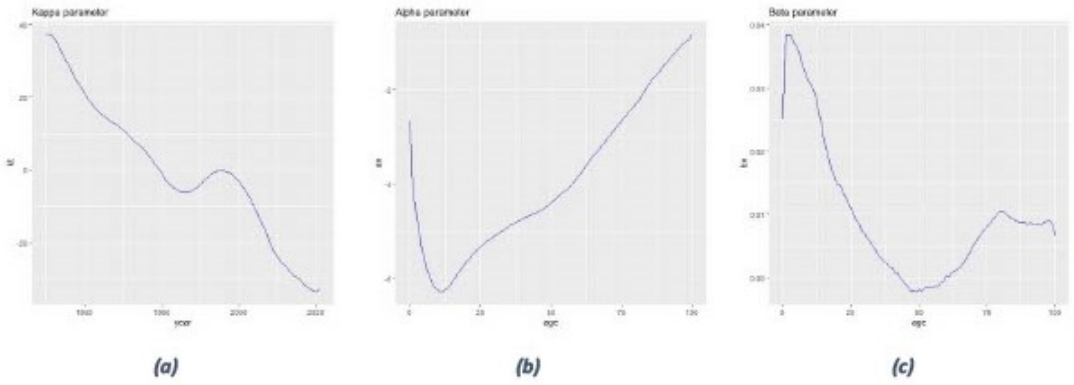

Fig. 5. Lee-Carter parameter estimates plot

The Lee- Carter model estimated is statistically significant with a log-likelihood score of -84543.7 of deviance 110405.2 and 272 parameters. The model explains 78.4% of the variation in the data set. The parameters estimate for the model are as shown in Fig. 5. General mortality pattern α is high for infant mortality, hump around ages of 25 years and linear increase from 50 years as shown in Fig. 5(c). The β parameter as shown Fig. 5(b), is low which is an indication of a uniform mortality rate change across years. However, from 44 to 59 years, the parameter β is negative which indicates worsening mortality in this age group over time. The mortality index $kappa_t$ declined in cubic way with two inflection points at approximately 1985 and 1995 respectively as shown in Fig. 5(a).

2.2.6 Forecast

The first step in forecasting mortality rate involves estimating future values of the mortality index (κ_t) parameter using ARIMA approach as described by Box and Jenkins [34]. The preferred model to fit in the forecast period

2022 to 2070 is ARIMA (1,1,0) with a drift given as;

$$\kappa_t = \kappa_{t-1} - 0.9873 + \epsilon_t \tag{2.53}$$

The model has a white noise of 0.0.915 standard deviation. The value of estimated κ_t parameter are as shown in Table 3.

Table 3. κ predicted values

year	2022	2023	2024	2025	2026	2027	2028	2029	2030	2031
κ	-33.717	-34.705	-35.692	-36.679	-37.667	-38.654	-39.641	-40.629	-41.616	-42.603
year	2032	2033	2034	2035	2036	2037	2038	2039	2040	2041
κ	-43.591	-44.578	-45.565	-46.553	-47.540	-48.527	-49.514	-50.502	-51.489	-52.476
year	2042	2043	2044	2045	2046	2047	2048	2049	2050	2051
κ	-53.464	-54.451	-55.438	-56.426	-57.413	-58.400	-59.388	-60.375	-61.362	-62.349
year	2052	2053	2054	2055	2056	2057	2058	2059	2060	2061
κ	-63.337	-64.324	-65.311	-66.299	-67.286	-68.273	-69.261	-70.248	-71.235	-72.223
year	2062	2063	2064	2065	2066	2067	2068	2069	2070	2071
κ	-73.210	-74.197	-75.184	-76.172	-77.159	-78.146	-79.134	-80.121	-81.108	-82.096

After estimating κ_t parameter, ASMR forecasts for h steps ahead are modeled using

$$ln(m_{x,t+h}) = \hat{\alpha_x} + \hat{\beta}_x \hat{\kappa_t} \tag{2.54}$$

The predicted ASMR are used to model life expectancy for the same period, with the result across age and year shown in Fig. 6.

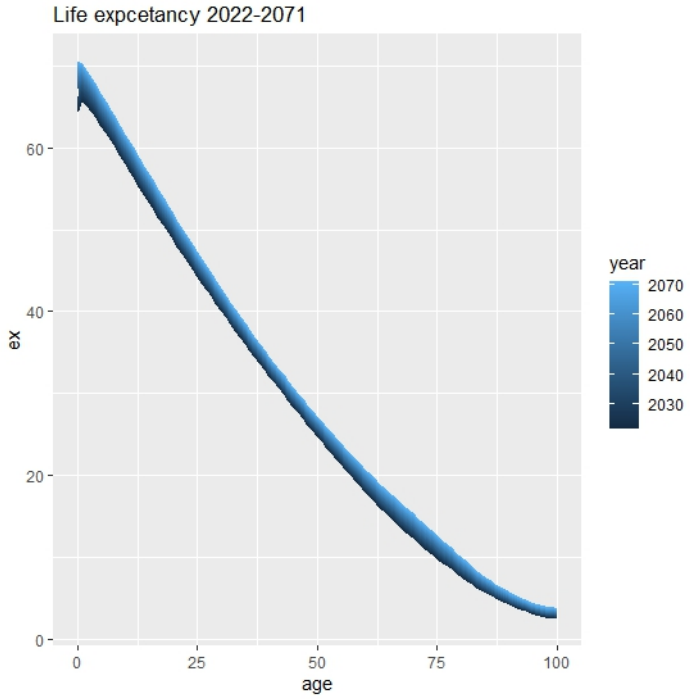

Fig. 6. Expected number of years left plot

Table 4. Forecast diagnostics

ERROR MEASURES BASED ON MORTALITY RATES			
Averages across ages			
ME	MSE	MPE	MAPE
-0.00019	0.00060	0.02092	0.11080
Averages across years			
IE	ISE	IPE	IAPE
-0.01537	0.04937	2.08505	11.06310

ME- mean error; MSE - mean square error; MPE- mean percent error; MAPE- mean absolute percent error; IE - integrated error; ISE- integrated square error; IPE- Integrated percent error and IAPE - integrated absolute percent error

To assess the accuracy of forecast, average error measure of mortality rate both across age and year are considered as shown in Table 4. Mean average percent error (MAPE) is used to tell how far off the predicted values are on average. On average across age, the predictions are less than 1% off the actual values. The average across years is slightly higher, at 11% off the actual values.

Generally life expectancy at any given age is projected to increase with time. Life expectancy at birth in 2022, 2023 and 2024 are 64.4, 64.5 and 64.7 respectively. Its projected that as Kenya attains a middle class developed country by 2030, life expectancy at birth would be 65.6 years.

3 Discussion and Conclusion

The study sort to analyses the trend and model mortality by considering life table functions, lifespan inequality, force of mortality and expected life expectancy at any given age. The life table functions demonstrated clear pattern in the characteristic of the life expectancy evolution, age distribution of death and modal age trend, and proportion of the population able to survive to a given age. Life expectancy at an exact given age has increased. Age-at death distribution showed a while infant mortality has continuously reduced in infant mortality with year 2020 having infant mortality rate of approximately 26 per 1000, which approximately equal to older age mode. The distribution also showed a slight reduction in modal age at death to 73 years in 2020 and a reduction in distribution dispersion. The Lorenz curve and Gini coefficient satisfactory exhibited the underlying pattern in lifespan inequality. Person year lived from birth to death are less equally distributed, with a slight improvement with time. The Gompertz and Lee-Carter model estimated were both statistically significant at 5% confidence level. Gompertz parameter estimates for the year 2021 were 0.0609 and 0.0035 for B and C respectively. The Malthusian parameter estimates indicate over the selected years, it's less than zero with slight improvements over time. Lee-Carter model indicated approximately uniform low mortality rate of change at any given year over time and a worsening mortality rate at the age of 44 to 59 years. For forecasting purposes, ARIMA(1,1,0) with a drift best fitted the data set in estimating the κ parameter used to predict expected mortality rate and life expectancy from year 2022 to 2070.

This study provides evidence to conclude that Kenya has experienced a shift in mortality status from a high mortality population, to an intermediate stage. Life expectancy and survival rate have significantly improved though lifespan inequality improvements are negligible. Deaths at exact age 25 is about 35 per ten thousand, with the rate death rate increasing by 6.09% per year starting from age 25. Under stable population assumptions, Kenya is a shrinking population and death rate decrease with increase in Malthusian parameter. Over the years, mortality factors have increased across age. Expected life expectancy at a given age is projected to increase, with life expectancy at birth in 2030 and 2071 being 65.6 and 70.5 years respectively.

We recommend that policy makers to consider developing measures and policy framework to address the worsening mortality at the age of 44 to 59, the spread of health risk factors across age and lifespan inequality. In addition, the child mortality measures being implemented be strengthen further as the population shift in

mortality status. For the period 1990 to 2020, mortality characteristics were worsening, we recommend future research to be undertaken to understand the drive force.

Competing Interests

Authors have declared that no competing interests exist.

References

[1] Roser M, Ortiz-Ospina E, Ritchie H. Life expectancy. Our world in data; 2013.

[2] Canudas-Romo V. The modal age at death and the shifting mortality hypothesis. Demographic Research. 2008;19:1179-1204.

[3] Canudas-Romo V. Three measures of longevity: Time trends and record values. Demography. 2010;47:299-312.

[4] Ouellette N, Bourbeau R. Changes in the age-at-death distribution in four low mortality countries: A nonparametric approach. Demographic Research. 2011;25:595-628.

[5] Horiuchi S, Ouellette N, Cheung SLK, Robine JM. Modal age at death: lifespan indicator in the era of longevity extension. Vienna Yearbook of Population Research. 2013;37-69.

[6] Basellini U, Camarda CG. Modelling and forecasting adult age-at-death distributions. Population studies. 2019;73(1):119-138.

[7] Shang HL, Haberman S. Forecasting age distribution of death counts: An application to annuity pricing. Annals of Actuarial Science. 2020;14(1):150-169.

[8] Bergeron-Boucher MP, Vázquez-Castillo P, Missov T. A modal age at death approach to forecasting mortality. SocArXiv; 2022.

[9] Cheung SLK, Robine JM, Tu EJC, Caselli G. Three dimensions of the survival curve: Horizontalization, verticalization, and longevity extension. Demography. 2005;42(2):243-258.

[10] Ebeling M, Rau R, Baudisch A. Rectangularization of the survival curve reconsidered: The maximum inner rectangle approach. Population Studies. 2018;72(3):369-379.

[11] Shkolnikov VM, Andreev EE, Begun AZ. Gini coefficient as a life table function: Computation from discrete data, decomposition of differences and empirical examples. Demographic Research. 2003;8:305-358.

[12] Vaupel JW, Zhang Z, van Raalte AA. Life expectancy and disparity: An international comparison of life table data. BMJ open. 2011;1(1):e000128.

[13] Giorgi GM, Gigliarano C. The Gini concentration index: A review of the inference literature. Journal of Economic Surveys. 2017;31(4):1130-1148.

[14] Zafeiris KN. Comparing the Mortality Regimes in 39 Populations. In Quantitative Demography and Health Estimates: Healthy Life Expectancy, Templates for Direct Estimates from Life Tables and other Applications. Cham: Springer Nature Switzerland. 2023;187-204.

[15] Lee RD, Carter LR. Modeling and Forecasting the Time Series of U.S. Mortality. Journal of the American Statistical Association. 1992;87(419):659–671.

[16] Lee RD, Rofman R. Modeling and forecasting mortality in Chile. Natas. 1994;22(59):182–313.

[17] Tuljapurkar S, Li N, Boe C. A universal pattern of mortality decline in the G7 countries. Nature. 2000;405(6788):789-792.

[18] Booth H, Maindonald J, Smith L. Applying Lee-Carter under conditions of variable mortality decline. Population studies. 2002;56(3):325-336.

[19] Carter LR, Prskawetz A. Examining structural shifts in mortality using the Lee-Carter method. Methoden und Ziele. 2001;39.

[20] Booth H, & Tickle L. The future aged: New projections of Australia.'s elderly population. Australasian Journal on Ageing. 2003;22(4):196-202.

[21] Lundström H, Qvist J. Mortality forecasting and trend shifts: An application of the Lee–Carter model to Swedish mortality data. International Statistical Review. 2004;72(1): 37-50.

[22] Debón A, Montes F, Puig F. Modelling and forecasting mortality in Spain. European Journal of Operational Research. 2008;189(3):624-637.

[23] Chavhan R, Shinde R. Modeling and forecasting mortality using the Lee-Carter model for Indian population based on decade-wise data. Sri Lankan Journal of Applied Statistics. 2016;17(1).

[24] Ibrahim NSM, Lazam NM, Shair SN. Forecasting Malaysian mortality rates using the Lee-Carter model with fitting period variants. In Journal of Physics: Conference Series. 2021;1988(1):012103

[25] Mubarik S, Wang F, Luo L, Hezam K, Yu C. Evaluation of Lee–Carter model to breast cancer mortality prediction in China and Pakistan. Frontiers in Oncology. 2023;13: 1101249.

[26] Carfora MF, Orlando A. A Preliminary Investigation of a Single Shock Impact on Italian Mortality Rates Using STMF Data: A Case Study of COVID-19. Data. 2023;8(6):107.

[27] Fazle Rabbi AM, Khan HT. Stochastic mortality forecasts for Bangladesh. Plos One. 2022;17(11):e0276966.

[28] United Nation. World population prospect; 2022.
Available: https://population.un.org/wpp/Download/Standard/Mortality/

[29] Keilman N. How accurate are the United Nations world population projections?. Population and Development Review. 1998; 24:15-41.

[30] Hanada, K. A formula of Gini's concentration ratio and its application to life tables. Journal of the Japan Statistical Society, Japanese Issue. 1983;13(2):95-98.

[31] Peltzman S. Mortality inequality. Journal of Economic Perspectives. 2009; 23(4):175-190.

[32] Gompertz, B. XXIV. On the nature of the function expressive of the law of human mortality, and on a new mode of determining the value of life contingencies. In a letter to Francis Baily, Esq. FRS &c. Philosophical transactions of the Royal Society of London. 1825; 115:513-583.

[33] Malthus TR. An essay on the principle of population. 1826;2.

[34] Box GEP, Jenkins GM. Time series analysis, forecasting and control. San Francisco, California: Holden-Day; 1976.

Peer-review history:
The peer review history for this paper can be accessed here (Please copy paste the total link in your browser address bar)
https://www.sdiarticle5.com/review-history/111814